

DOI:10.1002/ejic.201402043

Nonlinear Optical Properties of Conjugated Platinum(II) Acetylides with Multibranching Donor–Acceptor Structures

Puhui Xie,^{*[a]} Lingyu Wang,^[b] Zhaohui Huang,^[b] Fengqi Guo,^{*[b]} and Qiu Jin^[a]

Keywords: Donor-acceptor systems / Nonlinear optics / Platinum / Density functional calculations

Six conjugated platinum(II) acetylides with multibranching donor-acceptor structures (**1–6**) were synthesized. The absorption maxima of triazine-centered complexes **1–3** are red-shifted by 36–43 nm compared with those of triphenylamine-centered complexes **4–6**. The luminescence spectra of **4–6** in air-saturated chloroform showed one fluorescence peak and one phosphorescence peak. However, only one fluorescence peak was detected for **1–3** in air-saturated chloroform. The

transient absorption spectra of the compounds indicate the effective intersystem crossing from S_1 to T_1 . The nonlinear optical properties of **1–6** in *N,N*-dimethylformamide were studied using open Z-scan method. The results indicate that complexes **1** and **6** exhibit good nonlinear optical performance. The ratios of the effective nonlinear absorption cross section to ground-state absorption cross section $\sigma_{\text{eff}}/\sigma_0$ of complexes **1–6** are in the range of 4–22.

Introduction

Nonlinear optical materials have attracted significant interest because of their potential applications in electronic and optoelectronic areas such as optical data storage, optical limiting, photovoltaic devices, 3D microfabrication, microscopy and photodynamic therapy.^[1–10] Two significant conclusions from previous work can be made: (1) Molecules with donor-acceptor structures such as D–A, D–A–D, D– π –A, D– π –D, and multibranching structures generally exhibit excellent two-photon absorption properties, and the two-photon absorption cross sections can be increased by extending the molecular conjugated system or incorporating multidipole chromophores into the molecular structure.^[11–14] (2) Molecules containing heavy metal ions and rigid structures always exhibit large reverse saturable absorption due to the enhancement of the intersystem crossing from the first singlet excited state to the first triplet excited state.^[15,16] These conclusions can provide helpful guidelines for designing materials with large overall nonlinear optical properties.

Platinum(II) acetylide oligomers and polymers exhibit high, linear transmission over the visible region and strong reverse saturable absorption of the first triplet excited state

from the visible to infrared spectroscopic region because of the spin-orbit coupling interaction between the d orbital of the heavy Pt^{II} ion and the π orbitals of the ligands. Consequently, the reverse saturable absorption properties of some platinum(II) complexes have been studied extensively. However, the pioneering work done so far has mainly focused on the linear heavy metal atoms containing acetylides, and the relationship between the molecular structure and the nonlinear optical properties, especially the effect of the donor-acceptor structure on the nonlinear optical properties was not discussed.^[12,17–22] In recent years, the two-photon absorption phenomenon and the enhanced nonlinear absorption based on the absorption from both the singlet and triplet states of several platinum acetylides with linear dipolar geometry have been reported.^[23–26] In addition, it has been reported that the molecules with multipolar geometries could overcome the nonlinear optical efficiency/optical transparency trade-off and disfavor the centrosymmetric packing in the solid state, both of which have hampered the efficiency of quadratic nonlinear optical materials. Thus, lots of multibranching organic molecules were synthesized and their third-order nonlinear optical properties, especially the TPA properties, studied in recent years.^[27–33] The Humphrey group have synthesized a series of Ru-containing or multimetal-containing hyperbranched acetylide dendrimers, and testified that the dendritic alkynylruthenium complexes have a larger TPA cross-section than the corresponding linear model complexes, and that the nonlinear optical effect increases with an increase in the number of metal valence electrons.^[30] Although some multibranching platinum(II)-containing acetylides have been synthesized and studied, their nonlinear optical properties, especially the reverse saturable absorption properties, are seldom reported.^[33–35] The

[a] College of Sciences, Henan Agricultural University, Zhengzhou, Henan 450002, P. R. China
E-mail: phxie2013@163.com
<http://www.henau.edu.cn>

[b] College of Chemistry and Molecular Engineering, Zhengzhou University, Zhengzhou 450001, P. R. China
E-mail: fqguo@zzu.edu.cn
<http://www.zzu.edu.cn>

Supporting information for this article is available on the WWW under <http://dx.doi.org/10.1002/ejic.201402043>.

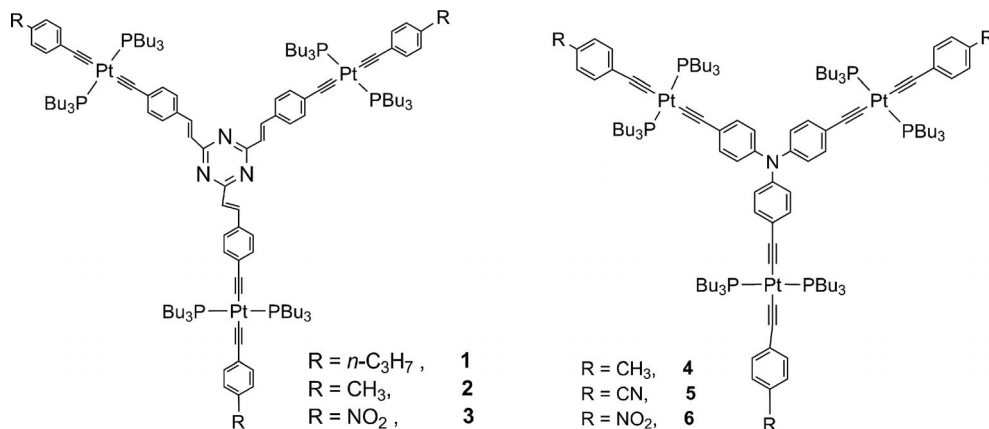


Figure 1. Structures of the multibranching conjugated trinuclear platinum(II) acetylide complexes.

detailed relationship between the structure and the two-photon absorption, as well as the excited state absorption, have still not been discussed clearly. Furthermore, how the two-photon absorption and the excited state absorption affect each other based on the structure of the complexes have also not been clearly discussed.

In order to address these questions, six multibranching platinum(II) acetylide complexes with donor-acceptor structures 1–6, as shown in Figure 1, were designed and synthesized. The design of the complexes is based on the well-known A– π –A, D– π –A and D– π –D motifs yielding materials with significant two-photon absorption. The insertion of the heavy metal atom into an organic molecule often results in materials with strong excited state absorption from the triplet state.^[16,32] Multibranching molecules consisting of a strong 1,3,5-triazine electron-accepting center or a strong triphenylamine electron-donating center have been shown to be excellent TPA materials, and the linked electron-donating or electron-accepting end groups, such as alkyl, nitro and nitrile, can enhance the extent of the electron delocalization of the molecules.^[29] The synthesized platinum acetylide complexes combine the donor-acceptor structure, multibranching structure and heavy metal in one molecule and this makes it possible to study the interaction between the two-photon absorption and the reverse saturable absorption based on the structure of the complexes. This paper will report the synthetic process, the photophysical properties and the nonlinear optical properties of the designed molecules for nanosecond lasers. The more detailed nonlinear optical properties for picosecond lasers and the relationship between the structure and nonlinear optical properties, as well as the interaction between two-photon absorption and reverse saturable absorption from the triplet state will be discussed in the future.

Results and Discussion

Quantum Calculations

The geometries of the platinum acetylides 2, 3, 4 and 6 were optimized. The HOMO and the LUMO were calcu-

lated using density functional theory (DFT) at the 6-31G(d) level for C, H, N, O and P, and at the LanL2DZ level for the Pt atoms. All the butyl groups in the molecules were replaced with the methyl groups in order to simplify the calculation process. The calculations were performed with the Gaussian 03 software package.^[36] The calculated electronic distribution situation is shown in Figure 2.

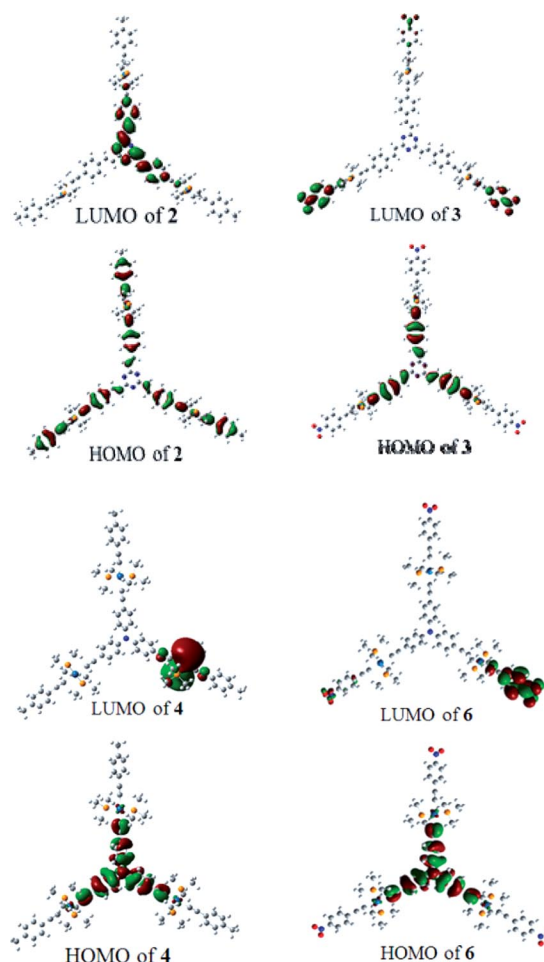


Figure 2. Electronic density distribution of the HOMO and LUMO orbitals of the platinum acetylides with multibranching donor-acceptor structures.

As shown in Figure 2, the electronic density of the HOMO of the triazine-centered complex **2** with the electron-pushing end is localized on the three branched chains with a clear contribution from Pt^{II}, whereas the electronic density of the LUMO of **2** is mostly located at the center of the molecule. The ligand-to-ligand (LLCT) and metal-to-ligand charge transfer (MLCT) clearly occur when the molecule is excited and the contribution of the metal $d\pi$ orbital to the LUMO is negligible compared with that in the HOMO. The electronic density of the HOMO of the triazine-centered complex **3** with the electron-withdrawing end is mostly localized on the arylacetyl groups between the triazine and the metal ion on the three branched chains with a slight contribution from Pt^{II} and the triazine group, whereas the electronic density of the LUMO of **3** is mostly located at the three electron-withdrawing arylacetyl groups on the end. The ligand-to-ligand (LLCT) charge transfer clearly occurs when the molecule is excited, and the contribution of the metal $d\pi$ orbital and the triazine centre to the LUMO is negligible compare with that in HOMO. The electronic density of the HOMO of **4** with a triarylamine center and electron-pushing ends on the three branched chains is located at the center with a clear contribution of the metal $d\pi$ orbital, whereas the electronic density of the LUMO is mostly located at the three metal ions. An obvious ligand-to-metal charge transfer (LMCT) happens when the molecule is excited. The electronic density of the HOMO of **6** with a triarylamine center and electron-withdrawing ends on the three branched chains is also located at the center with clear contribution of the metal $d\pi$ orbital, whereas the electronic density of the LUMO is mostly located at the three electron-withdrawing arylacetyl ending groups. The LLCT and metal-to-ligand charge transfer (MLCT) occur when the molecule is excited and the contribution of the metal $d\pi$ orbital to the LUMO is negligible. All the molecules exhibit conjugated systems after the insertion of Pt^{II} ions into the skeletons of them and the electron transfer process could occur by passing through the metal ions. In addition, the charge transfer behavior of these complexes should be dominated by the structures of the molecular skeletons. So it is possible to study the effect of heavy metal ions on the two photon absorption of the organic molecules with multibranching donor-accepter structures.

Electronic Absorption Spectra and Photoluminescence Spectra

The electronic absorption spectra of **1–6** in chloroform at $1 \times 10^{-5} \text{ mol L}^{-1}$ are shown in Figure 3 and the photophysical data are presented in Table 1. All the complexes exhibit absorption maxima in the range of 350–450 nm, attributed to the $\pi\text{--}\pi^*$ transitions. The absorption maxima of **1–3** are red-shifted by 36–43 nm when compared with those of **4–6** because of the larger conjugated systems of **1–3** relative to those in **4–6**. For the triazine-centered complexes **1–3**, the electronic push-pull properties of the *para* substituent on the phenyl acetylide do not affect their ab-

sorption maxima greatly, and the molar extinction coefficients increase with the increasing electron-withdrawing ability of the substituents. However, for the triphenylamine-centered complexes **4–6**, the electron-withdrawing group NO₂ makes the absorption maxima of **6** red-shifted by 5 nm compared with that of **4**. All the complexes showed weak absorption above 450 nm, which provides a wide observation window for the application in optical limiters.

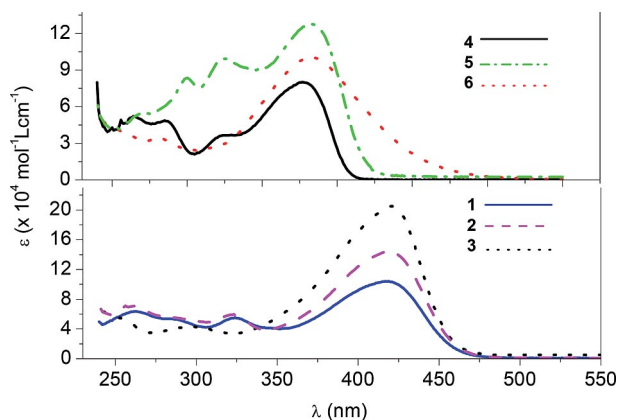


Figure 3. Electronic absorption spectra of compounds **1–6** in chloroform at $1.0 \times 10^{-5} \text{ mol L}^{-1}$ in a 1 cm cuvette.

Table 1. Photophysical properties of **1–6**.

	λ_{Abs} /nm	λ_{F} /nm	λ_{P} /nm	Stokes-shift /nm	ΔE_{S} /eV	τ_{em} /ns	τ_{TA} / μs
1	418	509	–	91	2.74	1.60 ^[a]	3.73
2	418	510	–	92	2.71	1.51 ^[a]	3.67
3	420	474	–	54	2.79	1.44 ^[a]	3.01
4	377	411	501	24	3.12	1.26 ^[a] 410 (69%) ^[b] 2761 (28%) ^[b]	1.50
5	382	420	547	38	3.07	1.28 ^[a] 545 (58%) ^[b] 3140 (38%) ^[b]	0.72
6	382	475	585	93	3.02	1.34 ^[a] 479 (78%) ^[b] 3700 (20%) ^[b]	

[a] Lifetime of fluorescence. [b] Lifetime of phosphorescence.

Figure 4 shows the excitation and luminescence spectra of complexes **1–6** in air-saturated chloroform. For the triazine-centered complexes **1–3**, the luminescence maxima are located at 510 nm, 509 nm and 474 nm, respectively, values which do not change in air-free chloroform solution and the responsible emissive lifetimes are in the range of 1.4–1.6 ns. These emissions can be attributed to the fluorescence from their first singlet excited states. The fluorescence maximum of **3** is blue-shifted by 35 nm compared with those of **1** and **2** because of the electron-withdrawing properties of the triazine and the NO₂ group. The low fluorescence quantum yields of 0.058, 0.058 and 0.0049 for **1**, **2** and **3**, respectively, indicate that the molecular population in the S_1 state relaxes mainly by means of intersystem crossing to the T_1 state or internal conversion to the ground state. However, the phosphorescence bands of **1–3** at room temperature were not observed in air-free chloroform. The

phosphorescence of some platinum acetylide complexes has only been observed at low temperature.^[37] In addition, the larger conjugated system of **1–3** relative to that in **4–6** decreased the coupling interaction between the ligands and the d orbital of Pt^{II}, and finally decreased the phosphorescence quantum yields of **1–3**. This is consistent with the reported results.^[38]

acetylide make both the fluorescence and phosphorescence maxima of **5** and **6** red-shifted compared with that in **4** with an electron-donating group at the end of the phenyl acetylide. The detectable room temperature phosphorescence spectra of **4–6** indicate that the heavy atom effect increases the intersystem crossing quantum yield. So it is possible for these molecules to possess great triplet excited state

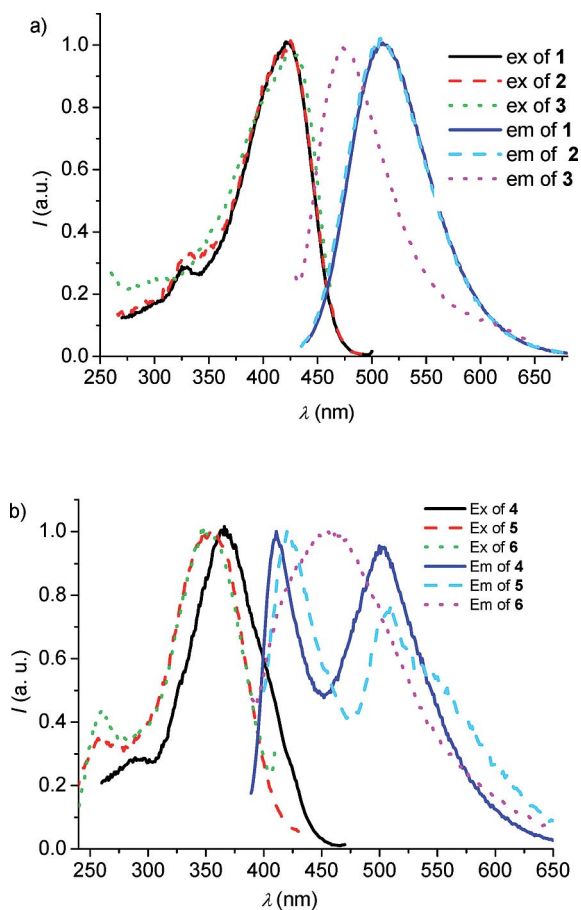


Figure 4. Normalized absorption and photoluminescence spectra in air-saturated chloroform solution of **1–3** (a) and **4–6** (b).

From the calculated results, the contribution of the metal $d\pi$ orbital in the LUMO of **1–3** is negligible and this also indicates the weak spin-orbital coupling effect.

The luminescence spectra of complexes **4–6** in air-saturated chloroform exhibit two main peaks (Figure 4, b and Figure 5). As shown in Figure 5, for each complex, the peak with the shorter wavelength, which becomes weak in the air-free solution and has a lifetime in the range of 1.26–1.34 ns, can be attributed to the fluorescence, and the peak with the longer wavelength, which becomes strong in air-free solution and has a lifetime in the range of 410–3700 ns, can be attributed to the phosphorescence. The detailed data are also listed in Table 1. The conjugated systems in **4–6** which are smaller than in **1–3** increase the coupling interaction between the ligands and the Pt^{II} d orbital and this makes the phosphorescence of **4–6** detectable at room temperature. For the triphenylamine-centered complexes **4–6**, the electron-withdrawing groups at the end of the phenyl

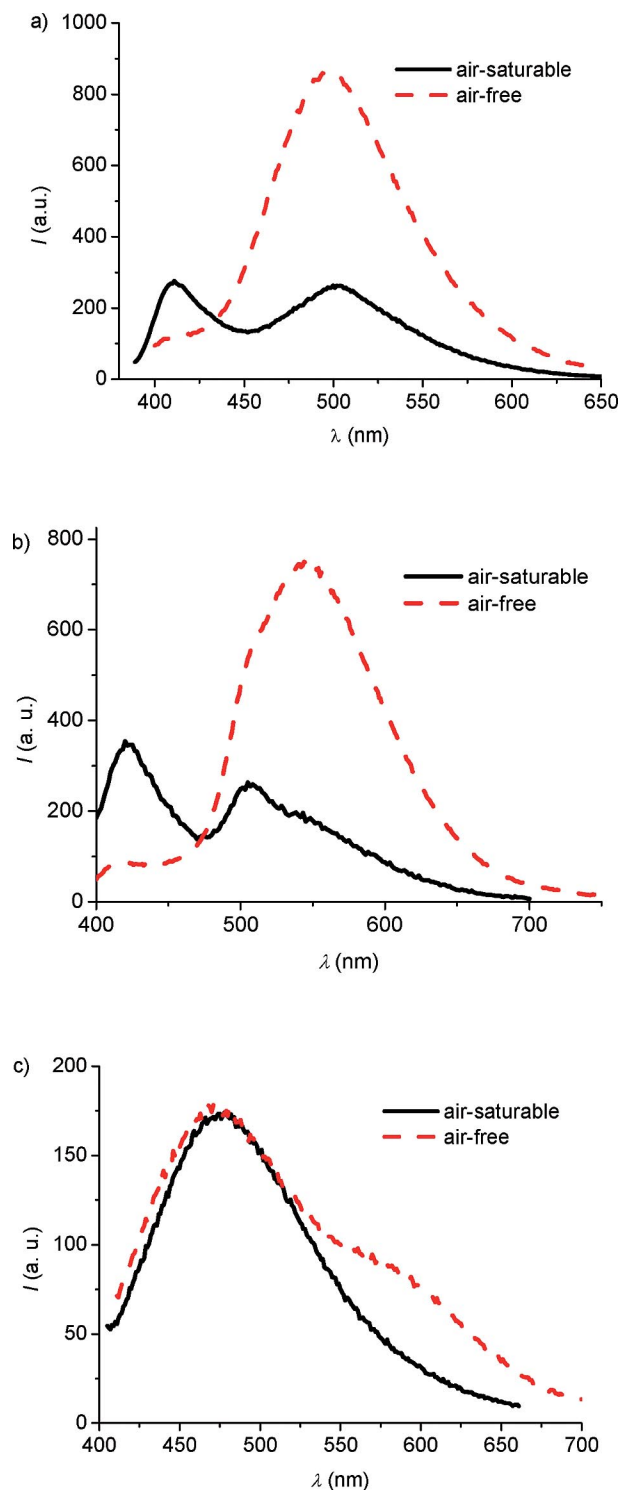


Figure 5. Photoluminescence spectra in air-saturated and air-free chloroform solutions of **4** (a), **5** (b) and **6** (c).

absorption. This is consistent with the reported results^[32] and the calculated results that the contribution of the metal $d\pi$ to the LUMO of **4-6** is effective. The phosphorescence bands of the synthesized complexes are significantly overlapping with the corresponding fluorescence bands so we did not calculate the quantum yields of the phosphorescence for complexes **4-6**.

Transient Absorption (TA) Spectroscopy

The time resolved transient absorption spectra are illustrated in Figure 6 for complexes **1-5**. Transient absorption of complex **6** was too weak to be observed. The TA spectra of **1, 2** and **3** show a similar strong absorption throughout the visible region with the maximum at around 610 nm and extending into the near-IR region. The τ_{TA} values of **1, 2** and **3**, as listed in Table 1, do not coincide with their τ_{em} values, which have been attributed to fluorescence lifetimes, indicating that the transient absorption arises from the triplet excited state. The strong transient absorption of **1, 2** and **3** shows that the intersystem crossing from S_1 to the T_1 state is effective and is consistent with the low fluorescent quantum yields of them. The TA spectra of **4** and **5** show a moderately intense narrow absorption band around 460 nm and a strong absorption band above 550 nm extending to the near-IR region. In addition, the τ_{TA} values coincide with τ_{em} values of the phosphorescence, indicating that the transient absorption arises from the same excited triplet state. In view of the calculated results and the similar appearance of the TA spectra to the other TA absorption of platinum(II) acetylide complexes, the transient absorption of the title complexes maybe represent the 3MLCT and $^3\pi,\pi^*$ excited states.^[18,39]

Nonlinear Absorption Properties

The nonlinear absorption behaviors of **1-6** in DMF were investigated using the open aperture Z-scan technique. As shown in Figure 3, **1-6** show very weak linear absorption at 532 nm, which provides a high transmittance at low incident laser energy. However, the weak linear absorption of the complexes at 532 nm makes the direct ground state to triplet state absorption possible, which may also contribute to the nonlinear optical absorption.^[40] In view of the fact that the $S_0 \rightarrow T_1$ transition is forbidden by normal spectroscopic selection rules, so the direct ground state to triplet state absorption is always insufficiently strong to build up the electron population of the T_1 state to a high level even if the spin selection rule can be broken. In addition, there should be a bleach signal in the wavelength region of 532 nm in the transient absorption spectrum if the direct ground state to triplet state absorption is the main mechanism to induce the nonlinear optical absorption of the T_1 state. However, there is no bleach in the transient absorption spectra (Figure 6). Thus, the nonlinear absorption properties should be attributed to the two-photon absorption from the ground state and the excited state absorption

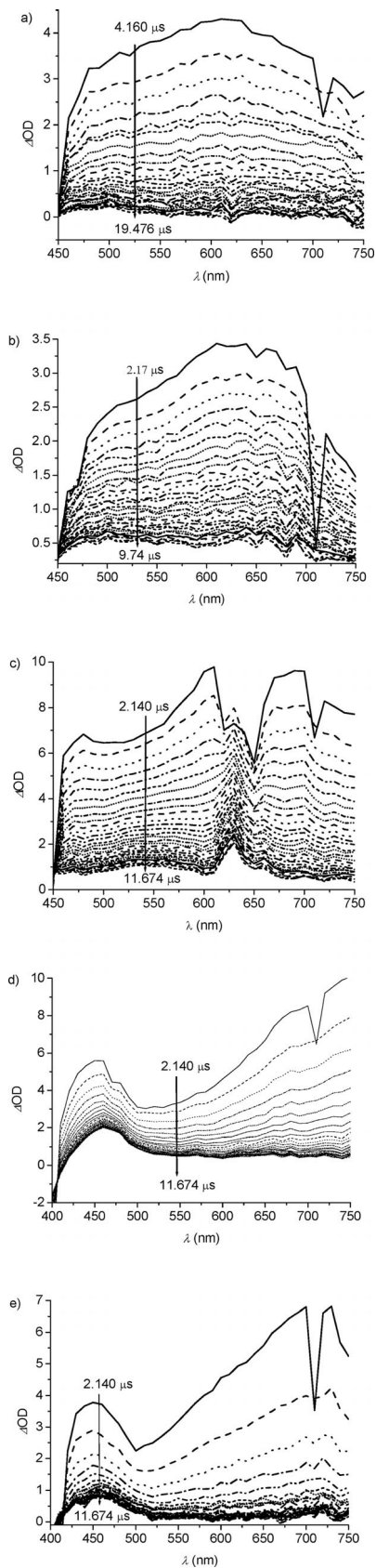


Figure 6. Transient absorption difference spectra of the title complexes **1** (a), **2** (b), **3** (c), **4** (d) and **5** (e) in nitrogen-degassed DMF solution at room temperature following 355 nm excitation. The arrows indicate the direction of the time decay.

from the first triplet excited state, which was induced by the two-photon absorption. The mechanism can be depicted by a simple five energy-level model as shown in Figure 7. The chromophore undergoes two-photon excitation from the ground state (S_0) to the first singlet excited state (S_1) or higher singlet excited state (S_n). The S_1 state can decay by means of the emissive path (F) or internal conversion (IC) to the ground state, or intersystem crossing (ISC) to the first triplet excited state (T_1). The T_1 state also can be excited to the higher excited triplet state, such as T_2 by absorbing another photon, or decay to the ground state by phosphorescence (P) or internal conversion (IC).

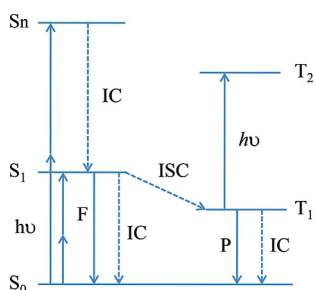


Figure 7. Five energy-level diagram for depicting the two-photon absorption from the first singlet excited state and the excited state absorption from the first triplet excited state induced by the two-photon absorption.

In order to compare the overall nonlinear optical properties of 1–6 but neglecting the detailed mechanism, the normalized transmittance data of the open aperture Z-scan were fitted according to the nonlinear absorption. In theory, it can be described by the following rate; see Equations (1), (2) and (3).^[41]

$$T = \ln\left(1 + \frac{q_0}{1+x^2}\right) / \left(\frac{q_0}{1+x^2}\right) \quad (1)$$

$$q_0 = \frac{\sigma_{\text{eff}} a_0 F_0 L_{\text{eff}}}{2h\nu} \quad (2)$$

$$L_{\text{eff}} = \frac{1 - e^{-a_0 L}}{a_0} \quad (3)$$

T is the normalized transmittance, $F_0 = E/(\pi\omega_0^2/2)$ is the on-axis laser fluency at the focus, E is the incident pulse energy, $x = z/z_0$, where z is the distance of sample from the focus and z_0 is the diffraction length of the beam, $z_0 = \pi\omega_0^2/\lambda$ where ω_0 is the beam waist at the focus; h is Planck's constant; L_{eff} is the effective sample thickness and L is the real sample thickness. The results from the Z-scan experiments are shown in Figure 8 in which the solid lines are theoretical fitting curves from Equation (1). As the sample was moved away from the focus point, the transmittances of all the complexes tended to an almost flat line which displayed the linear absorption under weak light irradiation. As the samples were moved close to the focus point, the transmittances decreased as the laser irradiance increased. At the focus point ($x = 0$) where the laser irradiance reached maximum, the normalized transmittance de-

creased to minimum. The open Z-scan data for 1–3 and 4–6 at a concentration of $5.0 \times 10^{-4} \text{ mol L}^{-1}$ in DMF solution are listed in Figure 8 (a and b), respectively, and the solid curve is the theoretical fitting. These results indicate that all of the complexes exhibit obvious nonlinear absorption properties. The ground state cross-sections, σ_0 , of complexes 1–6 are estimated at the magnitude of 10^{-18} cm^2 based on $\epsilon = 4.34 \times 10^{-4} \sigma_0 N_0$,^[42] in which ϵ is the molar absorption coefficient, N_0 is Avogadro's constant and σ_0 is the ground state absorption cross-section. The effective nonlinear absorption cross-sections (σ_{eff}) of the complexes were calculated by fitting the experimental data using Equation (1). The effective nonlinear absorption cross-sections and ground-state absorption cross-sections data of 1–6 are listed in Table 2. The magnitudes of the ground-state absorption cross-sections of 1–6 are of the order of 10^{-18} cm^2 , whereas the excited-state absorption cross-sections are of the order of 10^{-17} cm^2 at 532 nm. It is quite obvious that the efficient nonlinear absorption cross-sections are much larger than those of the ground state.

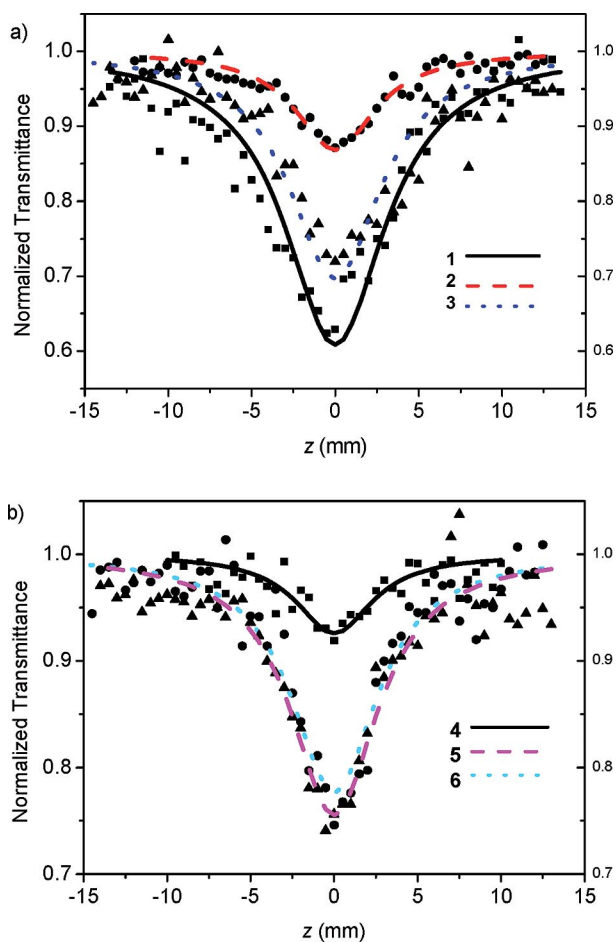


Figure 8. Open Z-scan data for 1–3 (a) and 4–6 (b) at a concentration of $5.0 \times 10^{-4} \text{ mol L}^{-1}$ in DMF solution. The solid curve is the theoretical fitting.

The ratio of $\sigma_{\text{eff}}/\sigma_0$ can be used to describe the overall nonlinear optical properties. For the triazine-centered complexes 1–3, the value of $\sigma_{\text{eff}}/\sigma_0$ increased with the electron

Table 2. The effective nonlinear absorption cross-sections of **1–6** in DMF.

	$\sigma_0 / 10^{-18} \text{cm}^2$	$\sigma_{\text{eff}} / 10^{-17} \text{cm}^2$	$\sigma_{\text{eff}}/\sigma_0$
1	3.72	8.21	22
2	3.94	1.61	4.1
3	7.96	2.52	3.2
4	2.43	1.34	5.5
5	5.74	2.19	3.8
6	2.93	4.85	16.6

pushing ability of the substitutes on the arylacetylide, and the value of $\sigma_{\text{eff}}/\sigma_0$ of **1** arrived at 22. Amongst the triphenylamine-centered complexes **4–6**, compound **6** with the strong electron-withdrawing $-\text{NO}_2$ substituent on the arylacetylide has the biggest $\sigma_{\text{eff}}/\sigma_0$ value of 16.6. However, **5** with a $-\text{CN}$ electron-withdrawing substituent on the arylacetylide only had a similar $\sigma_{\text{eff}}/\sigma_0$ value to complex **4** with the electron pushing $-\text{CH}_3$ substituent on the arylacetylide, probably because the conjugation effect of $-\text{CN}$ reduced the electron pulling effect of itself. From this result we can see that the multibranch conjugated platinum(II) acetylide complexes with a donor-acceptor structure have good overall nonlinear optical properties.

Conclusions

Three triazine-centered and three triphenylamine-centered multibranch conjugated platinum(II) acetylide complexes were synthesized. Their geometries were optimized and the HOMOs and LUMOs were calculated using DFT. The calculations show that all the molecules keep the conjugated system after the insertion of Pt^{II} ions into the skeletons and the electron transfer process could occur by passing through the metal ions. The charge transfer behaviors of these complexes should be dominated by the structures of the molecular skeletons. The low fluorescence quantum yields, detectable phosphorescence at room temperature and the time resolved transient absorption properties of them indicate that the intersystem crossing is effective. It is possible for the molecules to possess great triplet excited state absorption. The multibranch conjugated platinum(II) complexes exhibit good nonlinear optical performance and the overall nonlinear optical properties increase with an increase in the difference between the electronic pull-push ability between the center and the branch chromophores. More detailed research on how the two-photon absorption and the excited state absorption affect each other related to the structure of the complexes is going on in our lab and will be discussed in the future.

Experimental Section

Materials: All the starting materials from commercially available sources were used without any purification. All the solvents were dried and distilled by the standard methods. The details of the syntheses of the complexes **1–6** are given in the Supporting Information.

Methods: ^1H NMR spectra were recorded on a DRX-400 spectrometer and the chemical shifts are reported in ppm relative to TMS. MALDI-TOF mass spectra were measured on an AXIMA-CRF system. Elemental analyses were performed on a Flash EA 1112 analyzer. UV/Vis absorption spectra were measured on a TU-1901 spectrophotometer. The luminescence spectra were measured with a Cary Eclipse fluorescence spectrometer. The fluorescence quantum yields, Φ_f , were determined relative to quinine sulfate as the standard ($\Phi_f = 0.55$ in $0.5 \text{ N H}_2\text{SO}_4$).^[43] The emission lifetimes were measured on a FM-4P-TCSPC time-resolved fluorescence spectrometer. Transient absorption spectroscopy and transient absorption lifetimes were measured on an Edinburgh LP920 laser flash photolysis spectrometer. The samples were excited by the third-harmonic output (355 nm) of a Nd:YAG laser.

The open-aperture Z-scan measurements were performed with a diode-pumped pulse laser (Valiant 4 ω -100), which provides linearly polarized 16 ns optical pulses at 532 nm wavelength with a repetition of 100 Hz. The input laser beam was split into two beams by a beam splitter (Newport). One beam was employed as a reference to monitor the incident laser energy and the other was focused into the center of a 2 mm path-length sample cell by a 15 cm focal-length lens. The incident and transmitted laser pulses were monitored by two energy detectors, D1 and D2 (PE9-F and PE50 energy probes, Laser Precision), as reported.^[44] The measured diameter of the light spot at the focus was 50 μm . The concentrations of all the samples were $5.0 \times 10^{-4} \text{ mol L}^{-1}$ in DMF and samples were placed in a 2 mm path-length quartz cell.

Supporting Information (see footnote on the first page of this article): Details on the syntheses and characterization of the complexes **1–6**.

Acknowledgments

The authors thank the National Natural Science Foundation of China (NSFC) (grant number 21102037) and the Education Department of Henan Province (grant number 2010GGJS-048) for the financial support.

- [1] D. A. Parthenopoulos, P. M. Rentzepis, *Science* **1989**, *245*, 843–845.
- [2] A. S. Dvornikov, P. M. Rentzepis, *Opt. Commun.* **1995**, *119*, 341–346.
- [3] S. S. Chavan, B. G. Bharate, *Inorg. Chim. Acta* **2013**, *394*, 598–604.
- [4] R. Westlund, E. Malmstrom, C. Lopes, J. Ohgren, T. Rodgers, Y. Saito, S. Kawata, E. Glimsdal, M. Lindgren, *Adv. Funct. Mater.* **2008**, *18*, 1939–1948.
- [5] F. Dai, H. Zhan, Q. Liu, Y. Fu, J. Li, Q. Wang, Z. Xie, L. Wang, F. Yan, W.-Y. Wong, *Chem. Eur. J.* **2012**, *18*, 1502–1511.
- [6] F. Guo, Y. G. Kim, J. R. Reynolds, K. S. Schanze, *Chem. Commun.* **2006**, 1887–1889.
- [7] S. Achelle, P. Couleaud, P. Baldeck, M. P. Teulade-Fichou, P. Maillard, *Eur. J. Org. Chem.* **2011**, *76*, 1271–1279.
- [8] S. Kawata, H. B. Sun, T. Tanaka, K. Takada, *Nature* **2001**, *412*, 697–698.
- [9] W. Denk, J. H. Strickler, W. W. Webb, *Science* **1990**, *248*, 73–76.
- [10] J. D. Bhawalkar, N. D. Kumar, C. F. Zhao, P. N. Prasad, *J. Clin. Laser Med. Surg.* **1997**, *15*, 201–204.
- [11] H. Kim, B. Cho, *Chem. Commun.* **2009**, 153–164.
- [12] T. Lin, Y. Huang, Y. Chen, C. Hu, *Tetrahedron* **2010**, *66*, 1375–1382.
- [13] G. Zhou, W.-Y. Wong, C. Ye, Z. Lin, *Adv. Funct. Mater.* **2007**, *17*, 963–975.

- [14] X. Su, H. Xu, Q. Guo, G. Shi, J. Yang, Y. Song, X. Li, *J. Polym. Sci., Part A J. Polym. Sci. A: Polym. Chem.* **2008**, *46*, 4529–4541.
- [15] Y. Chen, L. Gao, N. He, J. Wang, Y. Araki, W. Blau, O. Ito, *Mini-Rev. Org. Chem.* **2009**, *6*, 55–65.
- [16] J. Zhao, W. Wu, J. Sun, S. Guo, *Chem. Soc. Rev.* **2013**, *42*, 5323–5351.
- [17] R. Zieba, C. Desroches, F. Chaput, M. Carlsson, B. Eliasson, C. Lopes, M. Lindgren, S. Parola, *Adv. Funct. Mater.* **2009**, *19*, 235–241.
- [18] F. Guo, W. Sun, Y. Liu, K. Schanze, *Inorg. Chem.* **2005**, *44*, 4055–4065.
- [19] J. E. McGarrah, R. Eisenberg, *Inorg. Chem.* **2003**, *42*, 4355–4365.
- [20] W. J. Blau, H. J. Byrne, D. J. Cardin, A. P. Davey, *J. Mater. Chem.* **1991**, *1*, 245–249.
- [21] A. P. Davey, H. J. Byrne, H. Page, W. Blau, D. J. Cardin, *Synth. Met.* **1993**, *58*, 161–172.
- [22] H. Page, W. Blau, A. P. Davey, X. Lou, D. J. Cardin, *Synth. Met.* **1994**, *63*, 179–182.
- [23] J. E. Rogers, T. M. Cooper, P. A. Fleitz, D. J. Glass, D. G. McLean, *J. Phys. Chem. A* **2002**, *106*, 10108–10115.
- [24] E. Glimsdal, M. Carlsson, B. Eliasson, B. Minaev, M. Lindgren, *J. Phys. Chem. A* **2007**, *111*, 244–250.
- [25] L. Liu, D. Huang, S. M. Draper, X. Yi, W. Wu, J. Zhao, *Dalton Trans.* **2013**, *42*, 10694–10706.
- [26] W. Wu, J. Zhao, J. Sun, L. Huang, X. Yi, *J. Mater. Chem. C* **2013**, *1*, 705–716.
- [27] S. K. Hurst, N. T. Lucas, M. G. Humphrey, T. Isoshima, K. Wostyn, I. Asselberghs, K. Clays, A. Persoons, M. Samoc, B. Luther-Davies, *Inorg. Chim. Acta* **2003**, *350*, 62–76.
- [28] C. E. Powell, J. P. Morrall, S. A. Ward, M. P. Cifuentes, E. G. A. Notaras, M. Samoc, M. G. Humphrey, *J. Am. Chem. Soc.* **2004**, *126*, 12234–12235.
- [29] Y. Jiang, Y. Wang, B. Wang, J. Yang, N. He, S. Qian, J. Hua, *Chem. Asian J.* **2011**, *6*, 157–165.
- [30] A. M. McDonagh, C. E. Powell, J. P. Morrall, M. P. Cifuentes, M. G. Humphrey, *Organometallics* **2003**, *22*, 1402–1413.
- [31] K. Onitsuka, A. Iuchi, M. Fujimoto, S. Takahashi, *Chem. Commun.* **2001**, 741–742.
- [32] A. M. McDonagh, M. G. Humphrey, M. Samoc, B. Luther-Davies, S. Houbrechts, T. Wada, H. Sasabe, A. Persoons, *J. Am. Chem. Soc.* **1999**, *121*, 1405–1406.
- [33] K. Onitsuka, M. Fujimoto, N. Ohshiro, S. Takahashi, *Angew. Chem. Int. Ed.* **1999**, *38*, 689–692; *Angew. Chem.* **1999**, *111*, 751.
- [34] C. E. Powell, M. P. Cifuentes, M. G. Humphrey, A. C. Willis, J. P. Morrall, M. Samoc, *Polyhedron* **2007**, *26*, 284–289.
- [35] S. Ghosh, P. S. Mukherjee, *Organometallics* **2008**, *27*, 316–319.
- [36] M. J. Frisch, G. W. Trucks, H. B. Schlegel, G. E. Scuseria, M. A. Robb, J. R. Cheeseman, J. A. Montgomery Jr., T. Vreven, K. N. Kudin, J. C. Burant, J. M. Millam, S. S. Iyengar, J. Tomasi, V. Barone, B. Mennucci, M. Cossi, G. Scalmani, N. Rega, G. A. Petersson, H. Nakatsuji, M. Hada, M. Ehara, K. Toyota, R. Fukuda, J. Hasegawa, M. Ishida, T. Nakajima, Y. Honda, O. Kitao, H. Nakai, M. Klene, X. Li, J. E. Knox, H. P. Hratchian, J. B. Cross, C. Adamo, J. Jaramillo, R. Gomperts, R. E. Stratmann, O. Yazyev, A. J. Austin, R. Cammi, C. W. Pomelli, J. Ochterski, P. Y. Ayala, K. Morokuma, G. A. Voth, P. Salvador, J. J. Dannenberg, V. G. Zakrzewski, S. Dapprich, A. D. Daniels, M. C. Strain, O. Farkas, D. K. Malick, A. D. Rabuck, K. Raghavachari, J. B. Foresman, J. V. Ortiz, Q. Cui, A. G. Baboul, S. Clifford, J. Cioslowski, B. B. Stefanov, G. Liu, A. Liashenko, P. Piskorz, I. Komaromi, R. L. Martin, D. J. Fox, T. Keith, M. A. Al-Laham, C. Y. Peng, A. Nanayakkara, M. Challacombe, P. M. W. Gill, B. Johnson, W. Chen, M. W. Wong, C. Gonzalez, J. A. Pople, *Gaussian 03*, revision B.05, Gaussian, Inc., Pittsburgh, PA, USA, **2003**.
- [37] L. Chen, A. H. Shelton, K.-Y. Kim, K. S. Schanze, *ACS Appl. Mater. Interfaces* **2011**, *3*, 3225–3238.
- [38] J. E. Rogers, J. E. Slagle, D. M. Krein, A. R. Burke, B. C. Hall, A. Fratini, D. G. McLean, P. A. Fleitz, T. M. Cooper, M. Drobizhev, N. S. Makarov, A. Rebane, K.-Y. Kim, R. Farley, K. S. Schanze, *Inorg. Chem.* **2007**, *46*, 6483–6494.
- [39] C. E. Whittle, J. A. Weinstein, M. W. George, K. S. Schanze, *Inorg. Chem.* **2001**, *40*, 4053–4062.
- [40] T. J. McKay, J. A. Bolger, J. Staromlynska, J. R. Davy, *J. Chem. Phys.* **1998**, *108*, 5537–5541.
- [41] G. L. Wood, M. J. Miller, A. G. Mott, *Opt. Lett.* **1995**, *20*, 973–975.
- [42] T. Xia, D. J. Hagan, A. Dogariu, A. A. Said, E. W. Van Stryland, *Appl. Opt.* **1997**, *36*, 4110–4122.
- [43] G. A. Crosby, J. N. Demas, *J. Phys. Chem.* **1971**, *75*, 991–1024.
- [44] M. Sheik-Bahae, A. A. Said, E. W. Stryland, *Opt. Lett.* **1989**, *14*, 955–957.

Received: February 11, 2014
Published Online: April 28, 2014